Color Doppler US of Renovascular Disease in Native Kidneys[1]

Olivier Hélénon, MD • Fadel El Rody, MD • Jean-Michel Correas, MD • Philippe Melki, MD, PhD • Dominique Chauveau, MD • Yves Chrétien, MD • Jean-François Moreau, MD

One hundred eighty-seven native kidneys in 96 patients were examined with color Doppler ultrasound (US) to (*a*) determine the color Doppler US characteristics of renovascular disorders and (*b*) assess the value of color Doppler US in detection of such disorders. Correlative angiography or computed tomography was performed in 94 patients. The following renovascular disorders were found: renal artery (RA) stenosis (40 cases), RA thrombosis (13 cases), RA aneurysm (four cases), renal vein thrombosis (three cases), arteriovenous fistula (three cases), peripheral infarction (one case of bilateral infarcts), and distal occlusive disease (three cases). One case of aortal coarctation was also found. Color Doppler US failed to demonstrate the proximal main RA in 25% of cases (among 193 RAs total including supernumerary RAs). The sensitivity and specificity of color Doppler US for the detection of RA stenosis or thrombosis were 89% and 99%, respectively. Color Doppler US thus appears to be effective in the diagnosis of renovascular disease in native kidneys.

■ INTRODUCTION

Duplex Doppler ultrasonography (US) is an interesting but controversial modality that enables diagnosis of renal artery (RA) stenosis (1–10). Owing to recent technologic improvements, there is increasing interest in use of color Doppler US for diagnosis of renovascular hypertension. By allowing real-time visualization of the renovascular tree, color Doppler US facilitates identification of the RA and allows direct analysis of hemodynamic changes. Therefore, color Doppler imaging has the potential to increase the accuracy of Doppler US in diagnosis of renovascular disease in native kidneys. However, because of the wide variability in performance in reported studies (11–13), color

Abbreviations: AV = arteriovenous, ESP = early systolic compliance peak–reflective wave complex, IVC = inferior vena cava, RA = renal artery, RI = resistive index, RV = renal vein

Index terms: Aneurysm, renal, 961.73 • Fistula, arteriovenous, 96.494 • Renal arteries, stenosis or obstruction, 961.721 • Renal arteries, thrombosis, 961.751 • Renal veins, thrombosis, 966.751 • Ultrasound (US), Doppler studies, 96.12983

RadioGraphics 1995; 15:833–854

[1] From the Departments of Radiology (O.H., F.E.R., J.M.C., P.M., J.F.M.), Nephrology (D.C.), and Urology (Y.C.), Hôpital Necker, 149 rue de Sèvres, 75743 Paris 15, France. Presented as a scientific exhibit at the 1993 RSNA scientific assembly. Received April 8, 1994; revision requested July 27 and received October 24; accepted October 25. **Address reprint requests to** O.H.

See the commentary by Berland following this article.

Doppler US needs further evaluation to determine diagnostic criteria and the appropriate scanning technique.

The purpose of the study described in this article was to correlate results of color Doppler US with results of angiography to determine the color Doppler US characteristics of renovascular disorders, including RA stenosis and thrombosis, RA aneurysm, renal vein (RV) thrombosis, arteriovenous (AV) fistula, peripheral infarction, and distal occlusive disease, and to assess the value of color Doppler US in detection of these disorders. A case of congenital narrowing of the aorta with severe renal hemodynamic abnormalities is also reported. This article also describes the normal color Doppler US appearance of the renal vasculature, presents limitations and pitfalls of color Doppler US, and discusses the diagnosis of common renovascular lesions with color Doppler US.

■ MATERIALS AND METHODS

In a 45-month period (May 1990 to January 1994), 187 native kidneys in 96 patients (58 men and 38 women with a mean age of 52 years [range, 17–82 years]) were examined with color Doppler US. Correlative angiography or computed tomography (CT) was performed in 94 patients. Eighty-five of the patients had hypertension, which was associated with renal failure in 24 patients. Renovascular hypertension was suspected on the basis of the usual clinical criteria, including accelerated hypertension, recent-onset hypertension, uncontrolled hypertension, malignant hypertension, severe hypertension in a young adult or a patient older than 50 years, renal failure, generalized arteriosclerotic occlusive disease, and the presence of an abdominal bruit. Five patients with persistent hypertension were examined after percutaneous transluminal angioplasty of an RA stenosis. In the 11 patients without hypertension, color Doppler US was performed for the following reasons: suspected RA occlusion following renal trauma (n = 2) or ex situ tumorectomy with autotransplantation (n = 1); acute renal failure (n = 5), which was associated with nephrotic syndrome in three cases; and severe postbiopsy hematuria (n = 3).

All lesions depicted with color Doppler US, except two of three postbiopsy AV fistulas, were also demonstrated with angiography or contrast material–enhanced CT. The results of color Doppler US were compared with the results of intraarterial digital angiography in 90 patients. Four patients (three with acute RV thrombosis and one with RA occlusion following renal trauma) underwent contrast-enhanced CT (Hilight Advantage; GE Medical Systems, Milwaukee, Wis) with 5-mm-thick contiguous sections.

Angiography was performed by means of a femoral artery approach with the Seldinger technique and a 5-F pigtail catheter. The degree of stenosis was calculated as follows: minimum diameter of the narrowed segment divided by the prestenotic diameter. The criterion for anatomically significant RA stenosis at angiography was 50% or greater RA narrowing (indicating a reduction of 75% or greater in cross-sectional area). Distal vascular lesions, including distal main RA stenosis, RA branch stenosis or thrombosis, RA aneurysm, peripheral infarction, and AV fistula, were demonstrated on selective renal angiograms.

Color Doppler US was performed with a Toshiba 270 SSA system (Toshiba Medical Systems Europe, Delft, The Netherlands) or an Hitachi EUB 565 system (Hitachi Medical, Tokyo, Japan) and a 3.75- or 3.5-MHz transducer with color and pulsed duplex Doppler capability. In addition, a 3.5-MHz phased-array sector transducer that provided color and continuous duplex Doppler sampling was used with the Toshiba system in most cases of RA stenosis to evaluate the accelerated systolic peak or to improve identification of the RA.

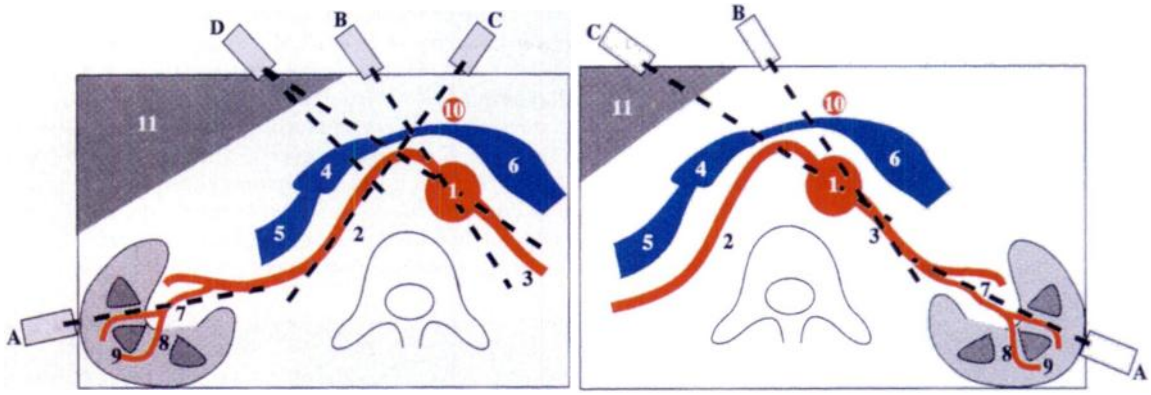

a. b.

Figure 1. Technique for duplex Doppler US examination of the RAs. *1* = aorta, *2* = right RA, *3* = left RA, *4* = inferior vena cava (IVC), *5* = right RV, *6* = left RV, *7* = segmental artery, *8* = interlobar artery, *9* = arcuate artery, *10* = superior mesenteric artery, *11* = liver. **(a)** Diagram shows examination technique for the right RAs. *A* = lateral scan (through the kidney) of the distal segment of the right RA and the RA branches; *B* = transverse anterior scan of the proximal segment of the right RA (see Fig 2a); *C* = transverse anterior scan of the middle segment of the right RA (see Fig 2a); *D* = lateral scan (through the liver) of the right renal pedicle (obtained when an anterior approach was unsuccessful) (see Figs 2c, 3) and longitudinal scan of the IVC and of the middle portion of the right RA as it courses posterior to the IVC (see Fig 4a). **(b)** Diagram shows examination technique for the left RAs. *A* = lateral scan (through the kidney) of the distal segment of the left RA and the RA branches (see Fig 2d); *B* = transverse anterior scan of the proximal and middle segments of the left RA (see Fig 2a, 2b); *C* = lateral scan (through the liver) of the proximal segment of the left RA (obtained when an anterior approach was unsuccessful) (see Fig 3).

Color Doppler US of the renal vessels was performed after gray-scale US of the kidney, adrenal gland, and renal pedicle. Gray-scale imaging was performed without preparation in fasting patients in the supine and posterior oblique positions. Doppler scanning of the renal vessels was performed with an anterior, right lateral, or posterolateral approach; the approach used depended on anatomic considerations (Fig 1). The peripheral intrarenal vasculature and the renal pedicle were first evaluated with color Doppler flow imaging.

The main RAs and at least three interlobar branches were also evaluated with pulsed duplex Doppler US. Spectral waveforms were obtained from the main RAs at an angle of insonation of less than 60°. The peak systolic velocity was evaluated in stenotic RAs; when the angle of insonation was greater than approximately 45°, the angle-corrected peak systolic velocity was evaluated.

Color Doppler US was performed and the results were interpreted by one (O.H.) or two (O.H. and F.E.R. or J.M.C.) investigators without knowledge of the results of CT or angiography.

Figures 2, 3. **(2)** Normal RAs. **(a)** Transverse anterior color Doppler sonogram shows the normal RAs (arrows). *Ao* = aorta, *LRA* = left RA, *RRA* = right RA. **(b)** Doppler spectrum (left) and color Doppler sonogram (right) of the left RA show a normal waveform. Note the aliasing phenomenon in the center of the lumen (arrow) owing to inadequate adjustment of the pulse repetition frequency. *Ao* = aorta. **(c)** Transverse oblique color Doppler sonogram (obtained with a lateral approach through the liver) demonstrates the whole course of the right RA (arrows) up to the renal hilum. Arrowhead = IVC, ★ = aorta. **(d)** Doppler spectrum (left) and color Doppler sonogram (right) of an intrarenal artery (straight arrow) show a normal waveform and a normal early systolic compliance peak (white curved arrow). Intrarenal arteries can be identified up to the arcuate branches (black curved arrow). **(3)** Normal RAs (lateral approach). Oblique longitudinal color Doppler sonogram obtained with the liver used as an acoustic window demonstrates the proximal portions of the RAs (arrows). On all Doppler sonograms, scale is in centimeters.

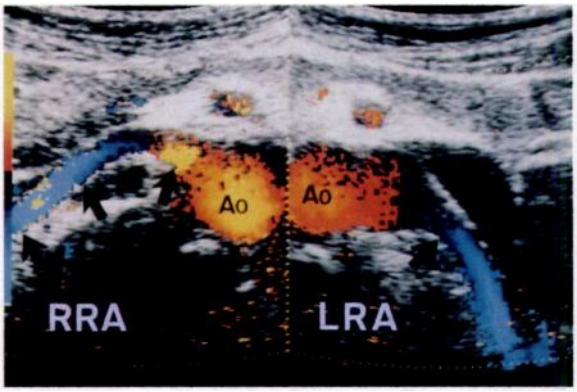

2a.

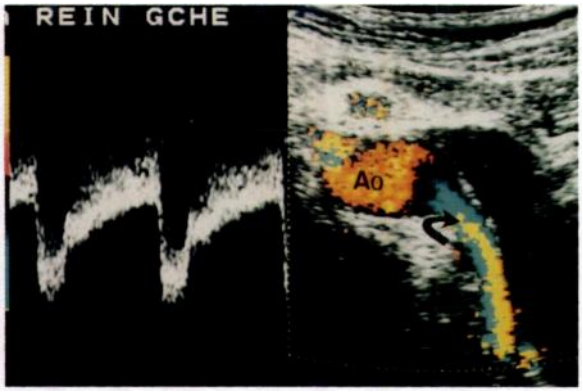

2b.

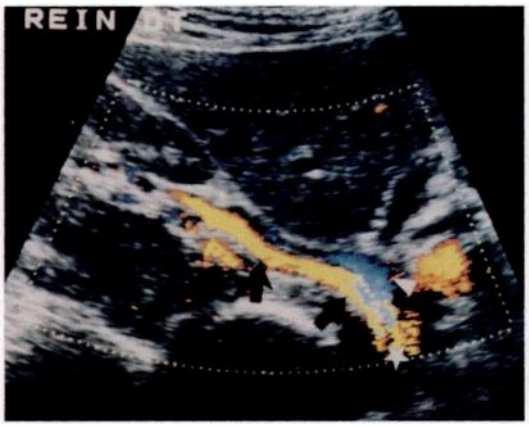

2c.

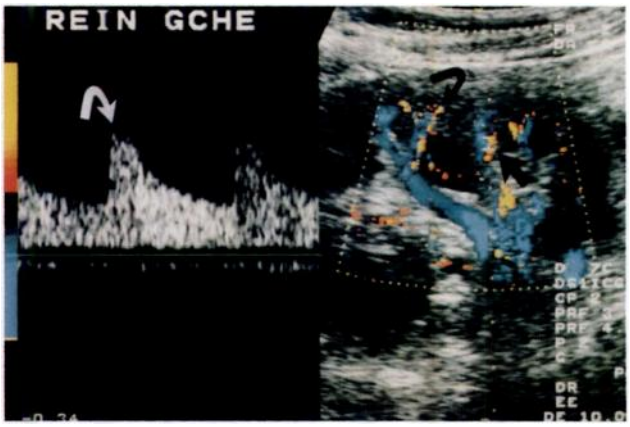

2d.

■ NORMAL ASPECTS AND PITFALLS

• Normal Renal Vasculature

Color Doppler US enables investigation of all levels of the vascular supply to native kidneys except vessels in the superficial cortex. Normal blood flow, as defined with color Doppler US and spectral analysis, can be depicted from the main RA to arcuate branches in the deep cortex (Figs 2–5).

Normal Doppler tracings obtained from intrarenal segmental or interlobar arteries show

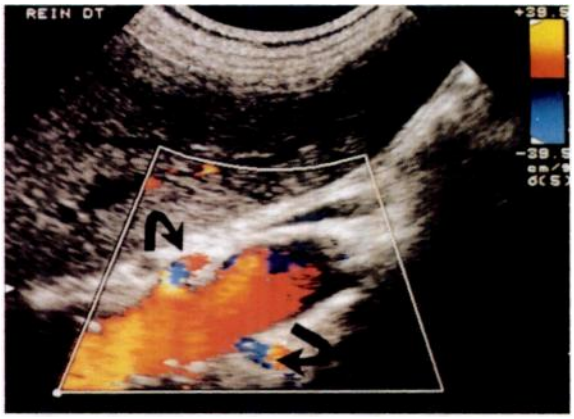

3.

Figures 4, 5. **(4)** Two RAs feeding the right kidney. **(a)** Longitudinal color Doppler sonograms show the middle segments of the RAs (white arrows) posterior to the IVC (★) (left) and the proximal segments of the RAs (black arrows) originating from the aorta (right). **(b)** Transverse anterior color Doppler sonograms show both right RAs (arrows). **(5)** Normal RVs. **(a)** Transverse oblique color Doppler sonogram obtained laterally demonstrates the right RV (arrowheads). **(b)** Transverse anterior color Doppler sonogram demonstrates the middle and distal segments of the left RV (solid straight arrows) up to the IVC (★). Note the lack of color Doppler signal in the distal segment of the vein (curved arrow) anterior to the aorta due to an inadequate angle of incidence. Open straight arrows = RAs. **(c)** Lateral color Doppler sonogram demonstrates the proximal segment of the left RV (arrow).

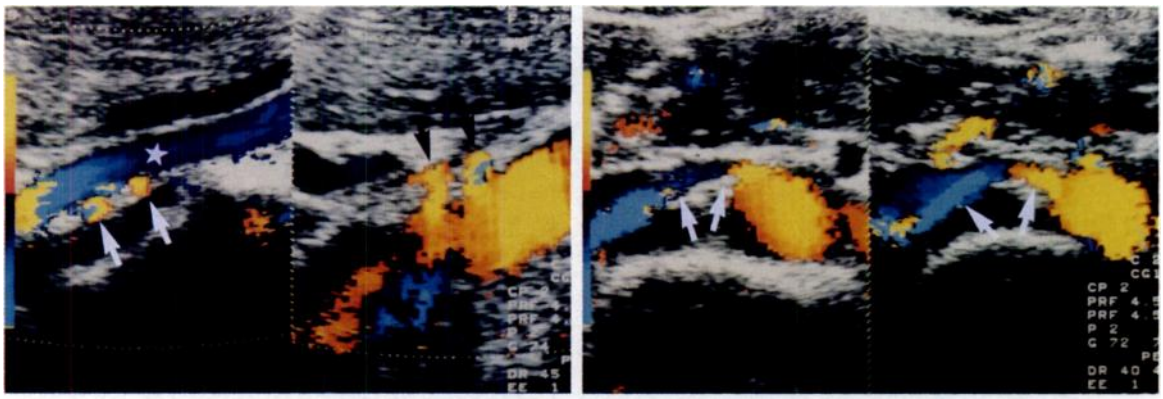

4a. 4b.

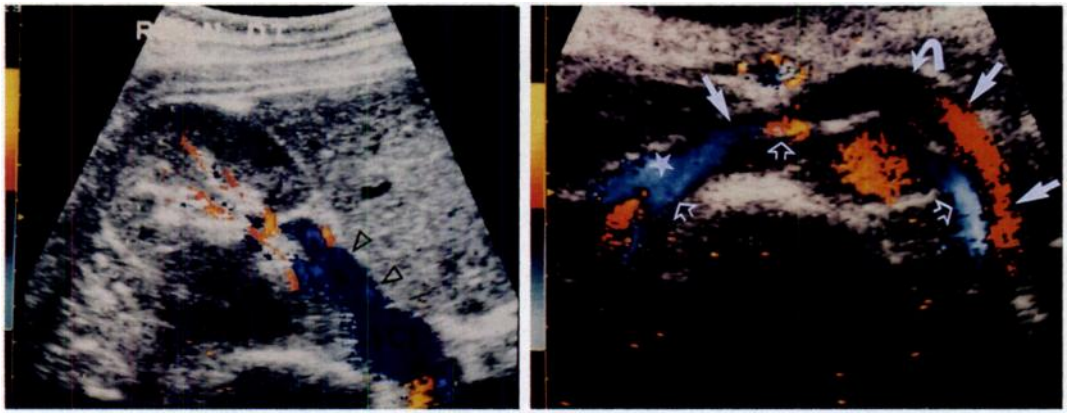

5a. 5b.

5c.

(*a*) marked systolic-diastolic modulation with a rapid (usually <0.07 seconds in segmental arteries) rise in systolic velocity up to at least 20–30 cm/sec and (*b*) an inconstant early systolic compliance peak–reflective wave complex (ESP) (Fig 2d). The more distal the location of the Doppler interrogation, the less frequent the presence of the ESP in normal intrarenal Doppler waveforms.

Parameters for Doppler waveforms obtained from intrarenal arterial branches include (*a*) the acceleration time of early systole (measured from the start of systole to the ESP), (*b*) the acceleration of the initial systolic upstroke (representing the slope of the initial systolic peak when angle-corrected velocity is used), (*c*) the resistive index (RI), and (*d*) the pulsatility index. The normal values for these parameters are somewhat ambiguous because the results of most studies that have evaluated such criteria in hypertensive patients are controversial (14–19).

Table 1
Color Doppler US Characteristics of RA Stenosis (40 Cases)*

Characteristic	Criteria	No. of Cases	Stenosis Grade (%)†
Acceleration at stenosis site	High systolic peak velocity‡	21	≥50 (50–95)
Poststenotic turbulence	Spectral broadening and reverse flow	21	≥50 (50–95)
	Color-coded turbulence	21	≥50 (50–95)
	Perivascular artifact	2	≥80 (80–90)
Downstream repercussions	Tardus-parvus waveform	7	≥80 (80–95)
All three characteristics	...	6	≥80 (80–95)

*Twelve of the 40 cases were missed with color Doppler US.
†Numbers in parentheses are ranges.
‡Velocity of 150 cm/sec or greater (range, 150–400 cm/sec).

• Limitations and Pitfalls

One of the major disadvantages of Doppler US is that accurate visualization of renal vessels can be compromised by anatomic factors related to patient corpulence or bowel gas. The right lateral approach, with the liver used as an acoustic window, is helpful in such cases (Figs 2c, 3), although the proximal and middle segments of the RA are usually scanned with the anterior approach.

Alterations in color encoding due to inadequate adjustment of technical parameters (particularly the pulse repetition frequency) or an inadequate angle of incidence of the ultrasound beam should be avoided when possible and not mistaken for an abnormality (Figs 2b, 5b).

Despite the advantages of color encoding, which is now widely available, technical success and accurate assessment of renal vessels require experience and a good knowledge of the normal RA blood supply, including (*a*) the collateral circulation—which may preserve distal perfusion in RA occlusion—and (*b*) congenital anomalies such as supernumerary RAs (Fig 4), retroaortic left RV (Fig 6), and circumaortic venous ring.

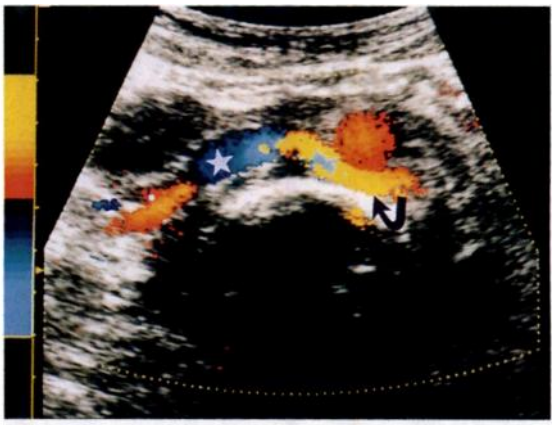

Figure 6. Retroaortic left RV. Transverse anterior color Doppler sonogram demonstrates the distal portion of a retroaortic RV (arrow) as it courses posterior to the aorta up to the junction with the IVC (★).

Identification of supernumerary RAs with color Doppler US requires careful, systematic scanning of the aorta with an anterior transverse approach. Longitudinal scanning of the IVC is also useful for identifying multiple right RAs running posterior to the IVC (Fig 4a). With this technique, supernumerary RAs are usually identified in patients with technically successful studies.

The presence of supernumerary RAs, as well as a well-developed collateral blood supply, can preserve normal downstream arterial flow in

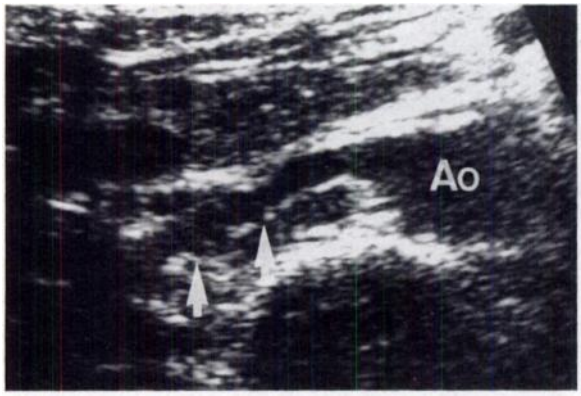

a.

b.

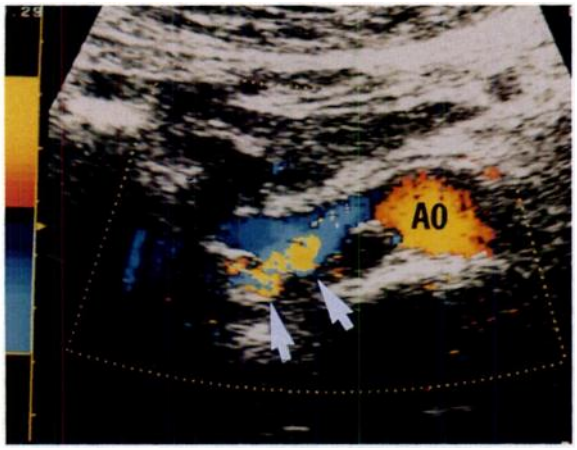

c.

Figure 7. Fibromuscular dysplasia. **(a, b)** Transverse sonogram **(a)** and angiogram **(b)** demonstrate the typical beady appearance of medial fibroplasia in the middle segment of the right RA (arrows). *Ao* = aorta. **(c)** Color Doppler sonogram demonstrates alteration of color encoding with aliasing phenomenon due to turbulence and acceleration of flow in the middle portion of the right RA (arrows). *AO* = aorta.

cases of severe stenosis (19). Moreover, arterial branches arising from a patent supernumerary RA could be sampled during Doppler interrogation, resulting in normal waveforms in cases of severe stenosis or even thrombosis involving the second main RA.

■ RESULTS

• RA Stenosis and Thrombosis

Sonographic Findings.—Real-time US can demonstrate abnormal appearances of the RA wall, such as (*a*) the typical beady appearance of the RA wall in medial fibromuscular dysplasia, as seen in three of four cases in our series (Fig 7a), and (*b*) thickening and calcification of the RA wall, which indicate an atherosclerotic lesion with calcified plaques but do not necessarily represent significant narrowing of the RA.

Color Doppler US Characteristics of RA Stenosis.—There were 40 cases of RA stenosis in our series (Table 1). The color Doppler US characteristics of RA stenosis included (*a*) ac-

Figure 8. Severe stenosis of the right RA. *Ao* = aorta. **(a)** Color Doppler sonogram demonstrates a perivascular artifact in the right RA (straight arrow). Note the normal appearance of the left RA (curved arrow). **(b)** Doppler spectrum obtained with continuous Doppler US at the site of the stenosis (left) shows a high systolic peak velocity of 300 cm/sec. On a color Doppler sonogram (right), there is also turbulence within the RA (arrows). **(c)** Doppler spectrum (left) obtained from the poststenotic segment shows marked spectral alteration with reverse flow due to turbulence. On a color Doppler sonogram (right), the poststenotic segment shows marked alteration of color encoding (arrow). **(d)** Angiogram shows a severe stenosis (arrow). **(e)** Arteriogram obtained after balloon angioplasty of the right RA shows improvement of the stenosis. **(f)** Doppler spectrum (left) and color Doppler sonogram (right) of the right RA 1 week after balloon angioplasty show a normal appearance.

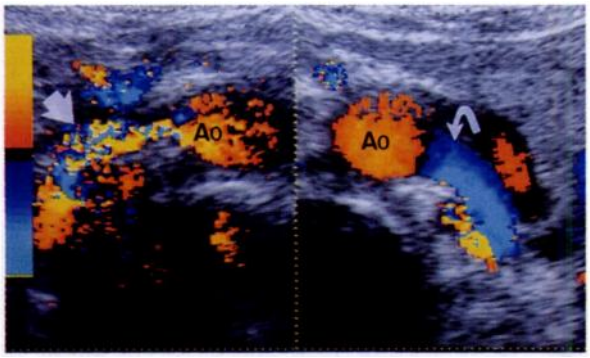

a.

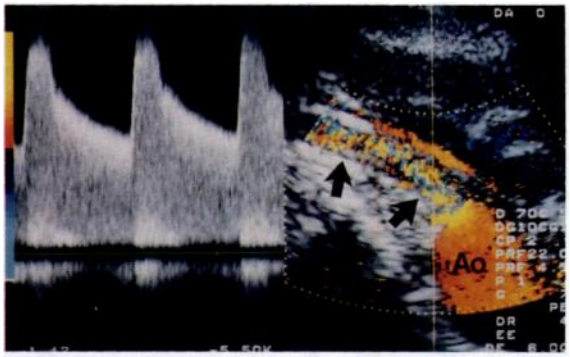

b.

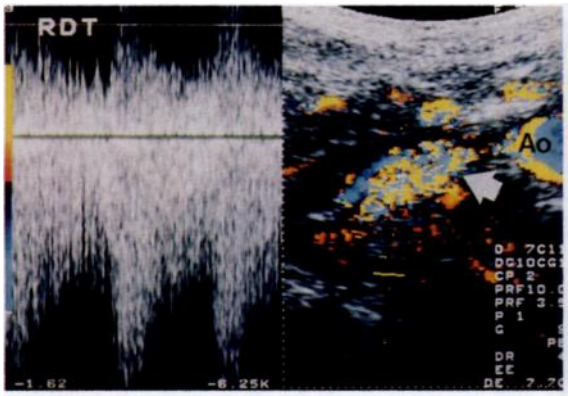

c.

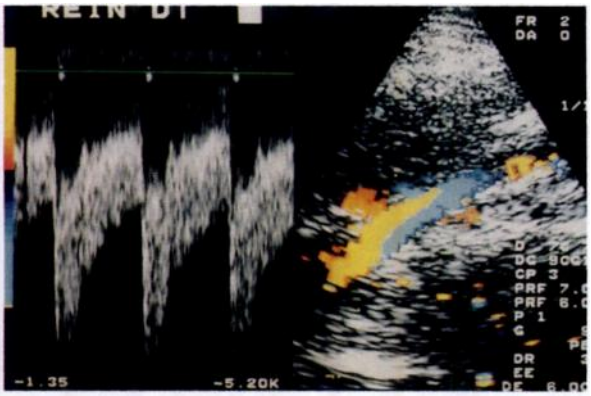

f.

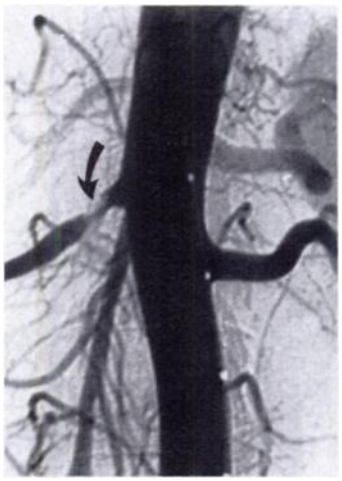

d.

e.

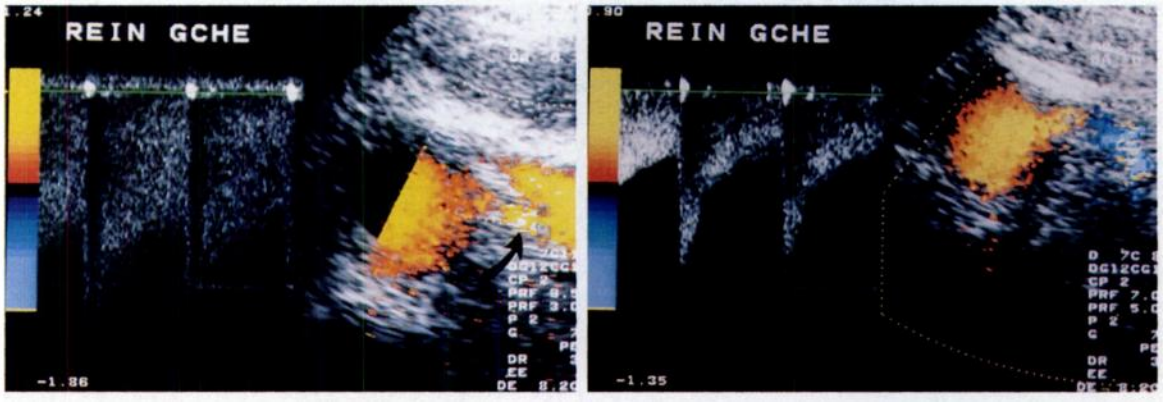

a. b.

c.

Figure 9. Severe stenosis of a supplementary left RA originating from the aorta. **(a)** Doppler spectrum (left) and color Doppler sonogram (right) of the superior left RA (arrow) demonstrate acceleration of flow (to at least 180 cm/sec). There was also poststenotic turbulence (not shown). **(b)** Doppler spectrum (left) and color Doppler sonogram (right) of the inferior left RA show a normal appearance. **(c)** Angiogram shows a severe stenosis of the superior left RA (arrow).

celeration at the site of stenosis (21 cases) (Figs 8b, 9a) with high systolic peak velocity (≥150 cm/sec for proximal lesions [range, 150–400 cm/sec]), resulting in color saturation toward white and aliasing phenomenon; (*b*) poststenotic turbulent flow (21 cases), seen as spectral broadening and alteration with reverse flow in all cases (Fig 8c) and resulting in intraluminal alteration of color encoding (Figs 7c, 8b) and occasionally in perivascular artifact (in two cases of severe stenosis of the main RA [5% of all cases of RA stenosis]) (Fig 8a); and (*c*) downstream repercussions induced by severe stenosis (13 cases), seen as a decrease in peak systolic velocity and a slower rise to peak systolic velocity with loss of normal systolic-diastolic modulation of Doppler waveforms, producing a smoother and smaller "envelope" (tardus-parvus Doppler waveform) than is normally seen in distal RAs (Fig 10).

The tardus-parvus pattern was observed in 13 of 17 cases of severe (≥80%) stenosis (range, 80%–95% stenosis). In one case, the tardus-parvus waveform was due to dual mild (both 70%) stenoses that involved the proximal and middle segments of the RA.

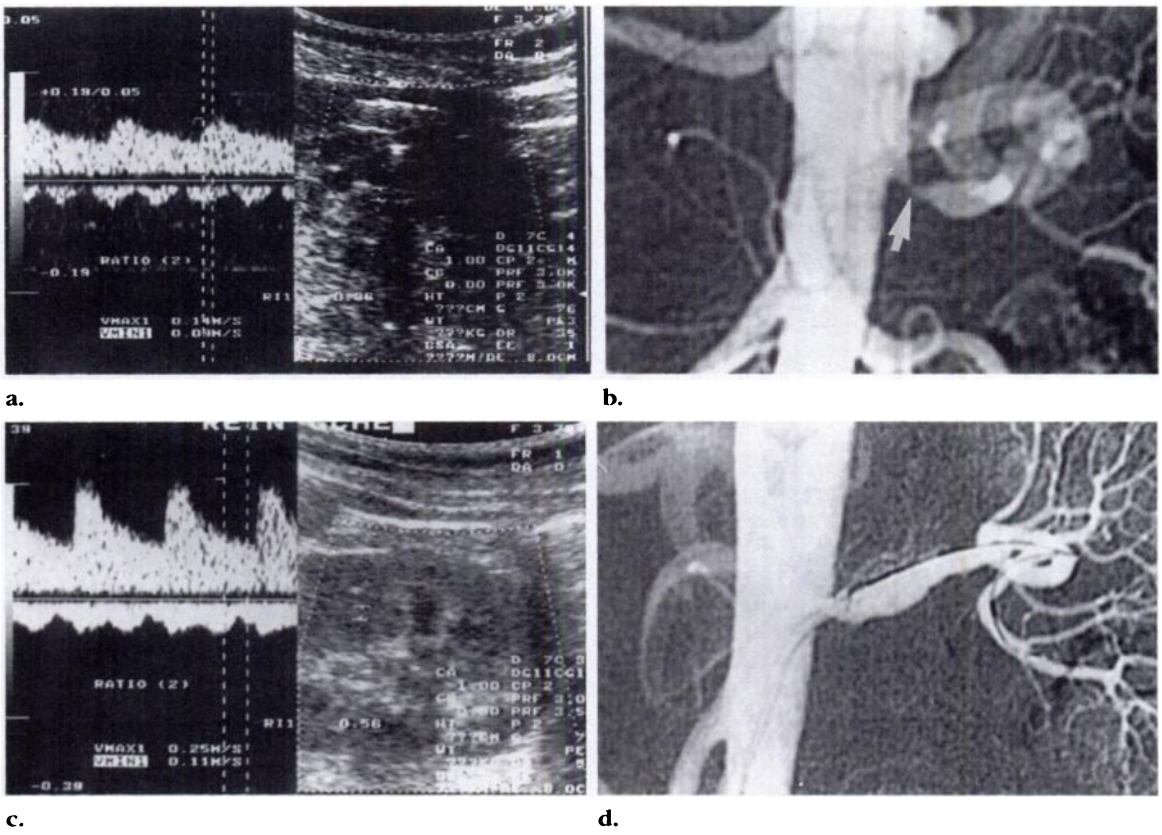

Figure 10. Severe stenosis with downstream repercussions. **(a)** Doppler spectrum (left) and sonogram (right) of the interlobar arteries show a tardus-parvus waveform due to downstream repercussions induced by a severe stenosis of the left RA. **(b)** Angiogram shows the severe stenosis of the left RA (arrow). **(c)** Doppler spectrum (left) and sonogram (right) obtained after balloon angioplasty of the left RA show improvement in distal renal arterial flow with normal systolic velocities. **(d)** Postangioplasty arteriogram shows improvement of the stenosis.

Table 2
Color Doppler US Characteristics of RA Thrombosis (13 Cases)*

Characteristic	Criteria	No. of Cases	Mechanism
Mute RA	Lack of signal in proximal RA	4	Atherosclerosis
	Presence of an arterial stump	2	Renal trauma
Downstream repercussions	Lack of intrarenal signal	8	Multiple causes†
	Tardus-parvus waveform	4	Atherosclerosis
Both characteristics	...	6	Multiple causes‡

*One of the 13 cases was missed with color Doppler US.
†Atherosclerosis in six cases and renal trauma in two cases.
‡Atherosclerosis in four cases and renal trauma in two cases.

In the four cases of severe stenosis (range, 80%–90% stenosis) without major downstream repercussions, the stenosis occurred in a kidney supplied by a single artery in three cases and in an upper polar supernumerary artery in the remaining case. In two of the three cases of a severely stenotic RA supplying the entire kidney, a decrease in RI and a prolonged acceleration time with loss of the ESP were noted retrospectively. In these two cases, the RI was 0.41 and 0.51, with a side difference of 0.12 or greater (0.18 and 0.12). In the remaining case, although the RI was 0.65, the presence of a congenital ureteropelvic junction obstruction (which required surgery) suggested a relative decrease in resistivity distal to the stenosis, since the RI should have been higher because of the chronic uropathy with an obstructed collecting system.

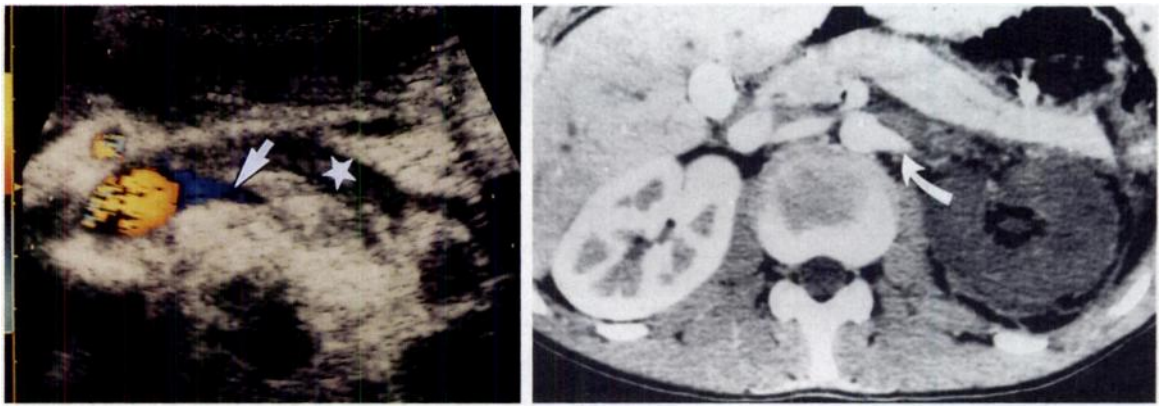

a. b.

Figure 12. RA occlusion following renal trauma. **(a)** Color Doppler sonogram shows occlusion of the left RA with an arterial stump (arrow). Note the concomitant RV thrombosis (★). **(b)** Contrast-enhanced CT scan shows proximal occlusion of the left RA (arrow) and a nonfunctioning, infarcted kidney.

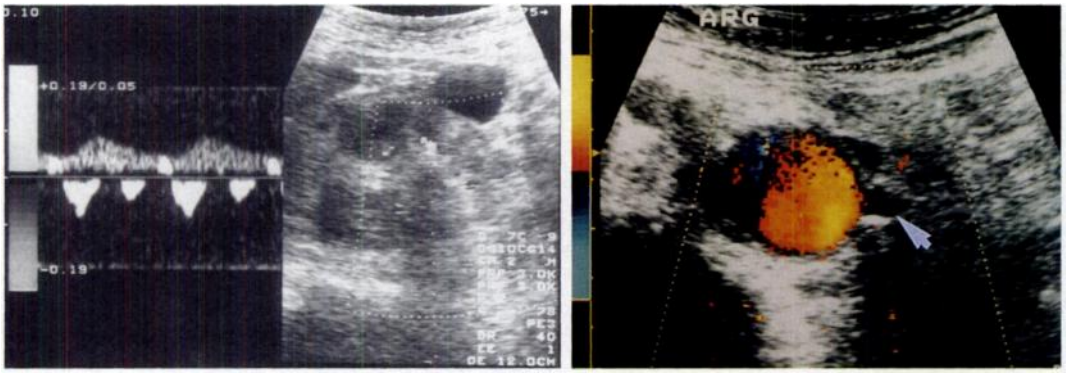

a. b.

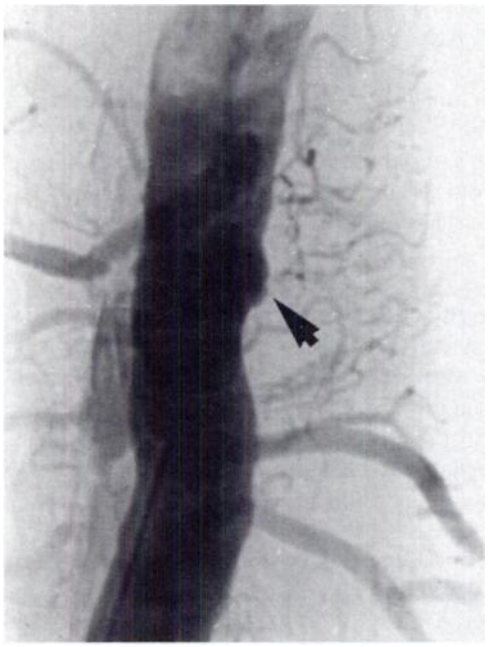

c.

Figure 11. RA thrombosis. **(a)** Doppler spectrum (left) and sonogram (right) of the segmental arteries of the left kidney show a severe tardus-parvus waveform. **(b)** Color Doppler sonogram shows that the proximal segment of the left RA is without flow (arrow). **(c)** Angiogram shows thrombosis of the left RA (arrow).

Color Doppler US Characteristics of RA Thrombosis.—There were 13 cases of RA thrombosis in our series (Table 2). In all 10 cases of thrombosis of the main RA, the thrombosis resulted in severe tardus-parvus abnormalities distal to the RA occlusion (two cases) (Fig 11a) or in lack of an intrarenal Doppler signal (eight cases). A mute RA (Fig 11b) or an arterial stump (Fig 12a) was visible on color Doppler images in six of 10 cases of main RA occlusion. In three cases, RA thrombosis developed in a renal arterial branch (two cases) or an ac-

Table 3
Color Doppler US Characteristics of RA Aneurysm (Four Cases)*

Type of Aneurysm	Criterion	No. of Cases	Diameter (mm)
Flowing	Hypoechoic mass filled with color Doppler signal	2	10 and 15
Calcified	Curved calcification	2	15 and 20
Thrombosed and calcified	...	1	20
Flowing and calcified	...	1	10

*Two of the four cases were missed with color Doppler US.

cessory supernumerary artery (one case). Color Doppler US demonstrated a segmental tardus-parvus pattern in two of these three cases (in the upper pole of the left kidney in one case and the lower pole of the left kidney in the other); in the remaining case (an arterial branch thrombosis), intrarenal Doppler interrogation did not demonstrate distal flow abnormalities (false-negative result).

Color Doppler US–Angiographic Correlation.—Color Doppler US did not enable visualization of proximal main RAs (193 RAs total including supernumerary arteries) in 25% of cases (48 RAs not identified). Six of 20 supernumerary arteries (30%) were identified at color Doppler examination prior to angiography.

With use of the above-mentioned criteria for diagnosing RA stenosis (localized hemodynamic abnormalities including increased blood flow velocity at the site of stenosis, turbulent blood flow just distal to the site of stenosis, or tardus-parvus waveform in the downstream circulation) and RA thrombosis (a mute RA and/or downstream repercussions including severe tardus-parvus abnormality or absence of detectable flow from distal intrarenal vessels), color Doppler US allowed detection of 37 of 48 cases of significant (≥50%) main RA stenosis (37 cases total) or thrombosis (11 cases total) and three of five cases of arterial branch stenosis (three cases total) or thrombosis (two cases total).

Of the 13 RA lesions (12 RA stenoses and one RA thrombosis) overlooked with color Doppler US, five lesions (including two segmental branch stenoses and one segmental branch thrombosis) were overlooked despite a technically successful examination (ie, there were five false-negative results). In the eight remaining cases, the color Doppler US examination was considered technically unsatisfactory, chiefly because the main RA or at least its proximal segment was not identified.

Six stenoses were found in renal arterial branches (three cases) or accessory supernumerary arteries (three cases). In these six cases, the color Doppler US examination was considered technically successful (ie, the main RA was identified) in four cases. Color Doppler US allowed diagnosis of two of these stenoses—one arterial branch stenosis and one supernumerary artery stenosis.

The overall sensitivity and specificity of color Doppler US for the detection of RA stenosis or thrombosis were 89% and 99%, respectively. Results of only the technically successful color Doppler US examinations were used to calculate false-negative results.

• RA Aneurysm

Two of four RA aneurysms (diameter range, 10–20 mm) were diagnosed with color Doppler US (Table 3). The aneurysms arose either from a renal arterial branch or distally from the main RA. Color Doppler US demonstrated a hypoechoic mass filled with color Doppler signal along the course of the RA in two cases (Fig 13). Spectral analysis showed turbulent flow within the aneurysms without the so-called to-and-fro feature. In two cases, flow within the cavity was not identified with color Doppler US because of peripheral calcification or aneurysmal thrombosis (false-negative result) (Fig 14). In one patient, a right renal arterial branch loop was misinterpreted as a small aneurysm (false-positive result); the results of CT and digital intravenous angiography were inconclusive. Intra-arterial angiography with selective angiography enabled us to rule out the presence of an RA aneurysm.

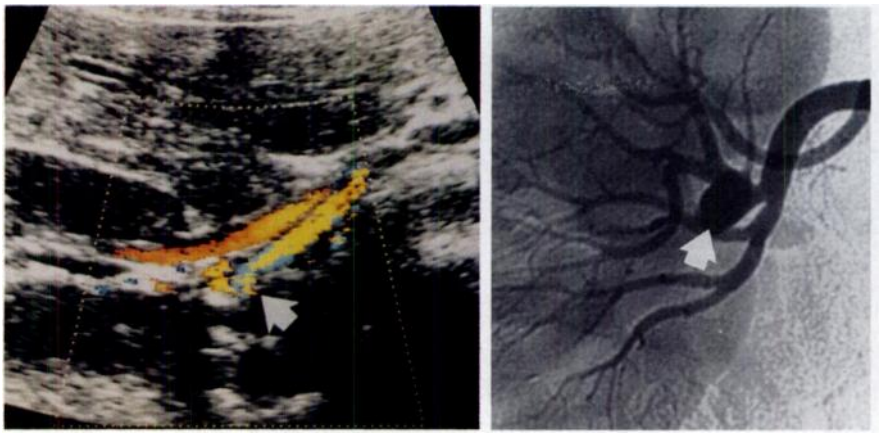

a. b.

Figure 13. RA aneurysm. **(a)** Color Doppler sonogram of the right renal hilum shows a small flowing mass filled with color Doppler signal (arrow). **(b)** Selective angiogram shows an aneurysm of a main renal branch (arrow).

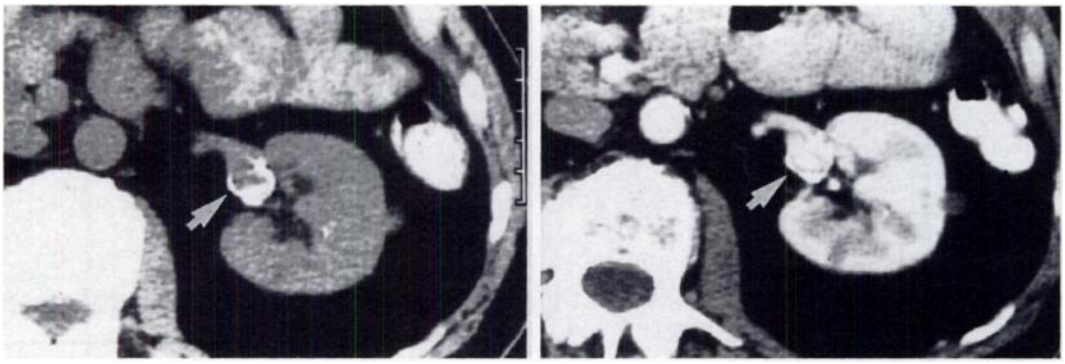

b. c.

a.

Figure 14. Calcified RA aneurysm. **(a)** Gray-scale sonogram demonstrates a curved calcification (arrow) with acoustic "shadowing" into the left renal hilum (arrowheads) but without detectable flow. **(b, c)** Nonenhanced **(b)** and contrast-enhanced **(c)** CT scans show a calcified, flowing aneurysm of the left RA (arrow). Scale in **b** is in centimeters.

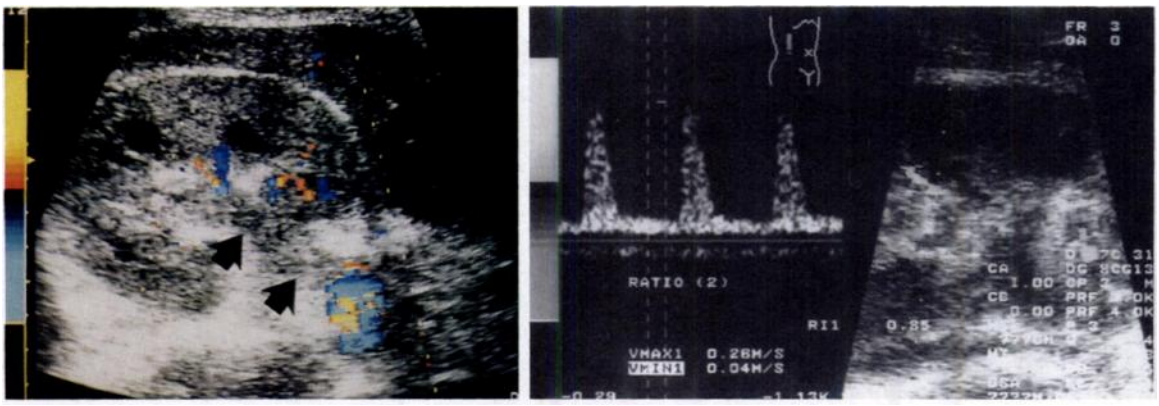

a. b.

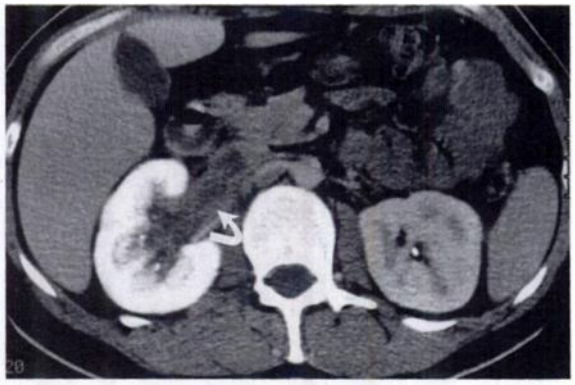

c.

Figure 15. Acute RV thrombosis accompanying nephrotic syndrome. **(a)** Color Doppler sonogram shows a mute, echogenic right RV (arrows). **(b)** Doppler spectrum (left) and sonogram (right) of the right RA demonstrate an increased RI of 0.85. **(c)** CT scan obtained after intravenous injection of contrast material shows a nonenhancing thrombus of low attenuation (arrow).

• RV Thrombosis

Three cases of acute RV thrombosis were diagnosed with color Doppler US and subsequently confirmed with CT. Color Doppler US showed a mute RV, with absence of blood flow noted on the color Doppler image and during pulsed Doppler interrogation. In all three cases, an echogenic thrombus was seen within the thrombosed vessel on gray-scale US images (Fig 15). In two of the three cases, spectral analysis showed no intrarenal venous flow abnormalities and increased RI values on Doppler tracings obtained from the RAs (Fig 15).

• Peripheral Renal Infarction

Multiple acute, bilateral, peripheral infarcts caused acute renal failure in one patient with acute pancreatitis. On color Doppler images and at duplex pulsed Doppler interrogation, large segmental infarcts showed complete loss of Doppler signal within hypoechoic areas of cortex shortly after infarction (Fig 16). The presence of multiple bilateral cortical defects was confirmed with selective angiography of both kidneys. Contrast-enhanced CT was useful in evaluating the anatomic extent of the infarction.

• Distal Occlusive Disease

Color Doppler US Characteristics.—There were two cases of severe arteriolonephrosclerosis and one case of polyarteritis nodosa, with no proximal lesion of the main RAs. In these cases, color Doppler US demonstrated bilateral inhomogeneous abnormalities of intrarenal Doppler waveforms, including tardus-parvus waveforms and abnormal spectra with increased systolic-diastolic velocities and decreased RI values obtained from interlobar arteries (Figs 17, 18). Microaneurysms were not visible on color Doppler images.

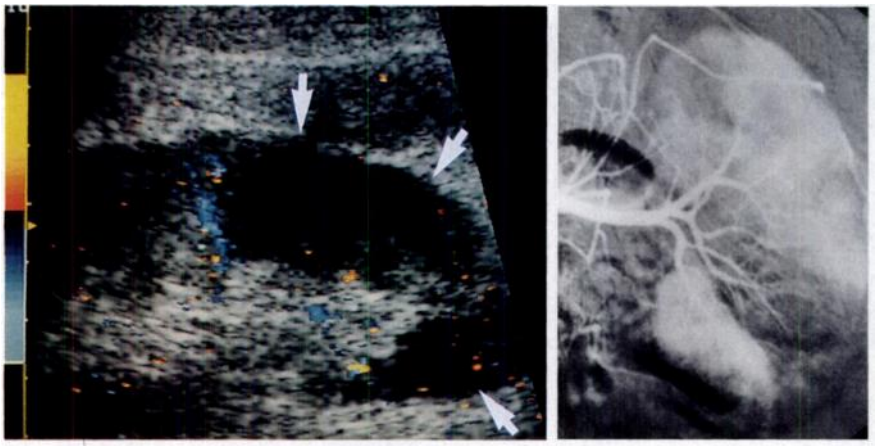

a. b.

Figure 16. Large cortical infarcts. **(a)** Color Doppler sonogram shows hypoechoic areas without flow (arrows). **(b)** Selective angiogram of the left kidney demonstrates multiple cortical defects comparable with those of the opposite side (not shown).

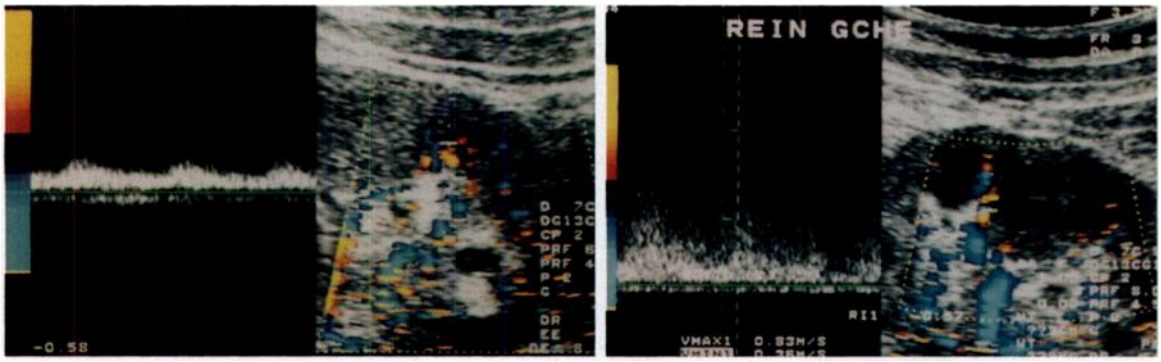

a. b.

c.

Figure 17. Severe arteriolonephrosclerosis. **(a, b)** Doppler spectrum (left) and color Doppler sonogram (right) of distal intrarenal arterial branches in the left kidney show inhomogeneous abnormalities of waveforms related to marked slowing of flow in poststenotic or reperfused arterial segments **(a)** and to acceleration of flow with turbulence in narrowed branches **(b)**. The same findings were demonstrated in the right kidney (not shown). **(c)** Selective angiogram of the left kidney demonstrates typical distal occlusive disease with prominent capsular collateral vessels (black arrowheads) supplying blood to the outer cortex. Note the inhomogeneity of cortical perfusion with obliteration of some distal interlobar arteries (white arrowheads). The same findings were demonstrated in the right kidney (not shown).

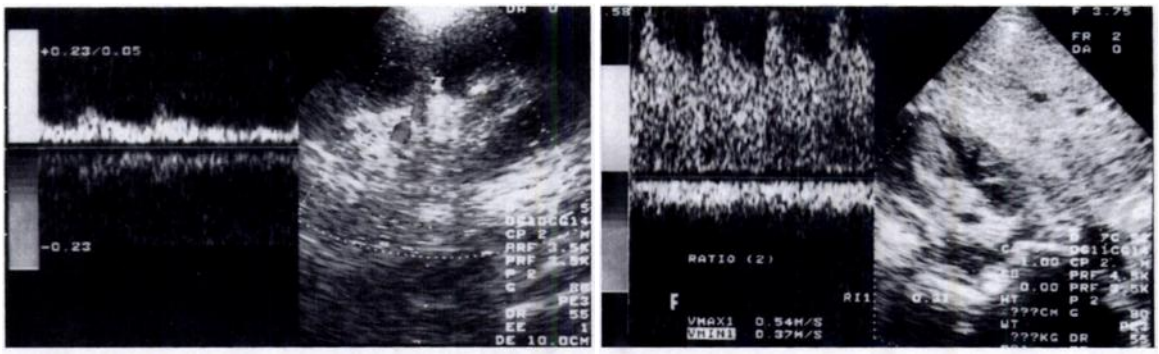

a. b.

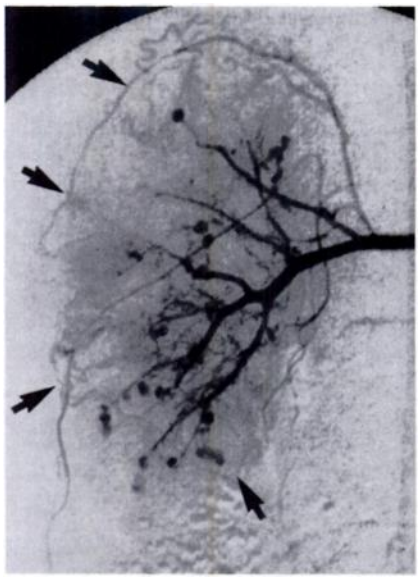

c.

Figure 18. Polyarteritis nodosa. **(a, b)** Doppler spectrum (left) and sonogram (right) of the segmental and interlobar arteries of the right kidney show inhomogeneous hemodynamic alterations including a severe tardus-parvus waveform **(a)** and accelerated low-resistance flow **(b)**. Microaneurysms were not visible on the color Doppler sonograms. **(c)** Selective angiogram of the right kidney demonstrates multiple aneurysms of the interlobar arteries, characteristic of a necrotizing arteritis. Also note the inhomogeneity of cortical perfusion, with prominent capsular arteries supplying small branches to the renal cortex (arrows).

Color Doppler US–Angiographic Correlation.—The inhomogeneous alteration of intrarenal blood flow seen with color Doppler US correlated with angiographic abnormalities involving the distal renovascular bed. Such angiographic abnormalities included pruning and irregularity of interlobar and arcuate vessels; inhomogeneity of cortical perfusion with marked slowing of flow; enlarged, sinuous intrarenal collateral pathways and prominent capsular arteries; and microaneurysms (in polyarteritis nodosa) (Figs 17c, 18c).

• Postbiopsy AV Fistula

In two of three postbiopsy AV fistulas, a focal perivascular artifact was observed at the site of the fistula (Figs 19, 20). Such an artifact was not observed in one case examined shortly after the biopsy (Fig 21). There was color saturation toward white and aliasing phenomenon, reflecting the increase in flow velocity in the artery supplying the fistula and in the draining vein. Aneurysmal dilatation of the draining vein was observed in two long-standing AV shunts with a large perivascular artifact extending into the renal hilum (Fig 20). Typically, AV shunts have three characteristics at spectral analysis: (*a*) accelerated, highly turbulent flow at the site of the shunt; (*b*) increased systolic-diastolic flow velocity with markedly decreased RI values (0.30–0.40) in the feeding artery; and (*c*) increased flow velocity with systolic-diastolic modulation in the draining vein. A venous flow arterialization pattern and decreased arterial resistivity may also be seen at the level of the renal pedicle in large, high-flow AV fistulas, as in one case in our series (Fig 20).

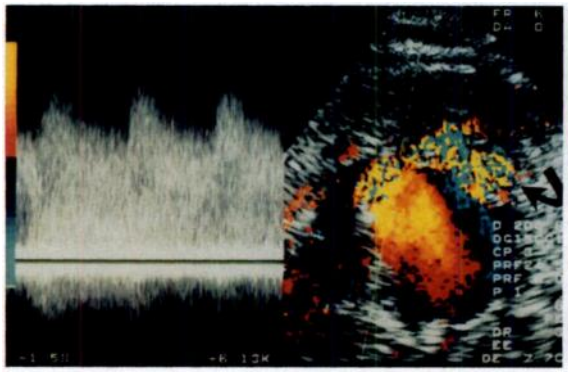

19.

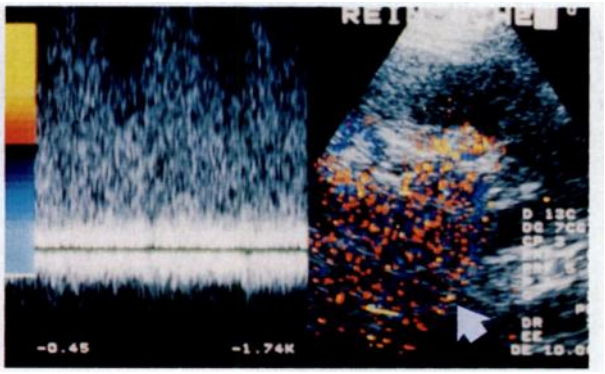

20a.

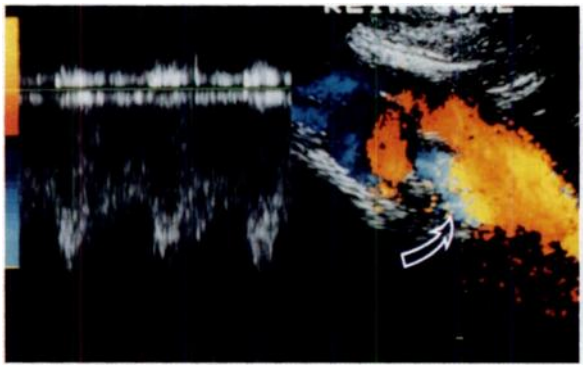

20b.

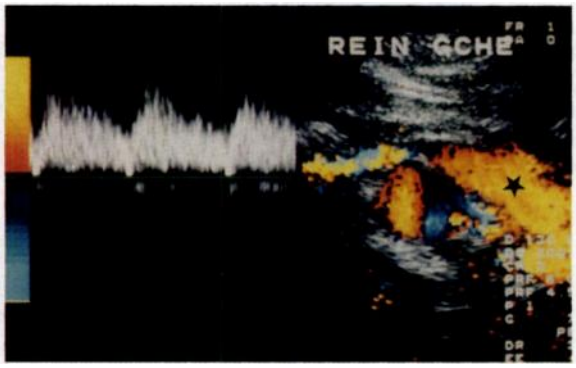

20c.

Figures 19, 20. **(19)** Postbiopsy AV fistula. Doppler spectrum obtained from the supplying artery (left) and color Doppler sonogram (right) demonstrate increased systolic and diastolic flow velocities and a decreased RI of 0.30, as well as a perivascular artifact related to extravascular tissue vibration at the site of an AV fistula (arrow). **(20)** Large AV fistula. **(a)** Doppler spectrum obtained from the feeding artery (left) and color Doppler sonogram (right) show a large perivascular artifact extending into the renal hilum (arrow) and a typical waveform. **(b)** Doppler spectrum (left) and color Doppler sonogram (right) show hemodynamic abnormalities in the main RA (arrow) with a decreased RI of 0.38. **(c)** Doppler spectrum (left) and color Doppler sonogram (right) show hemodynamic abnormalities in the RV (★), which was enlarged and demonstrated unusual pulsatility.

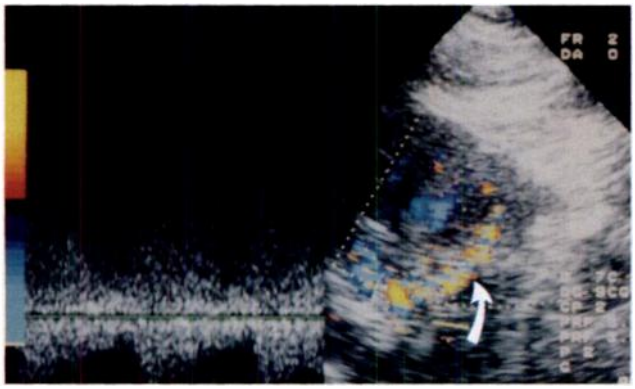

a.

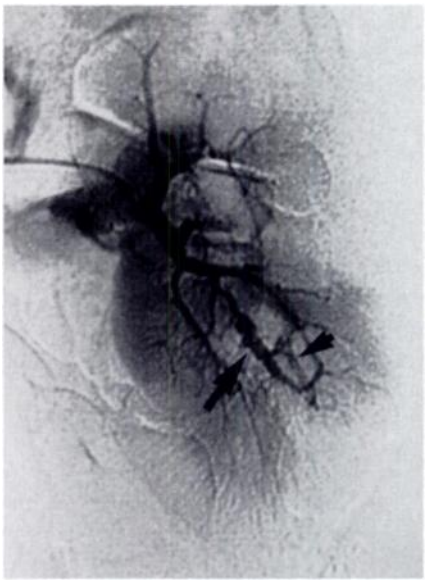

b.

Figure 21. Small AV fistula examined shortly after biopsy. **(a)** Doppler spectrum (left) and color Doppler sonogram (right) demonstrate spectral broadening and acceleration of flow with increased venous flow velocity and pulsatility. There is accelerated, turbulent flow in an interlobar branch without perivascular artifact (arrow). **(b)** Superselective renal angiogram shows a small AV fistula with an enlarged, tortuous feeding arterial branch (long arrow) and an early-filling draining vein (short arrow).

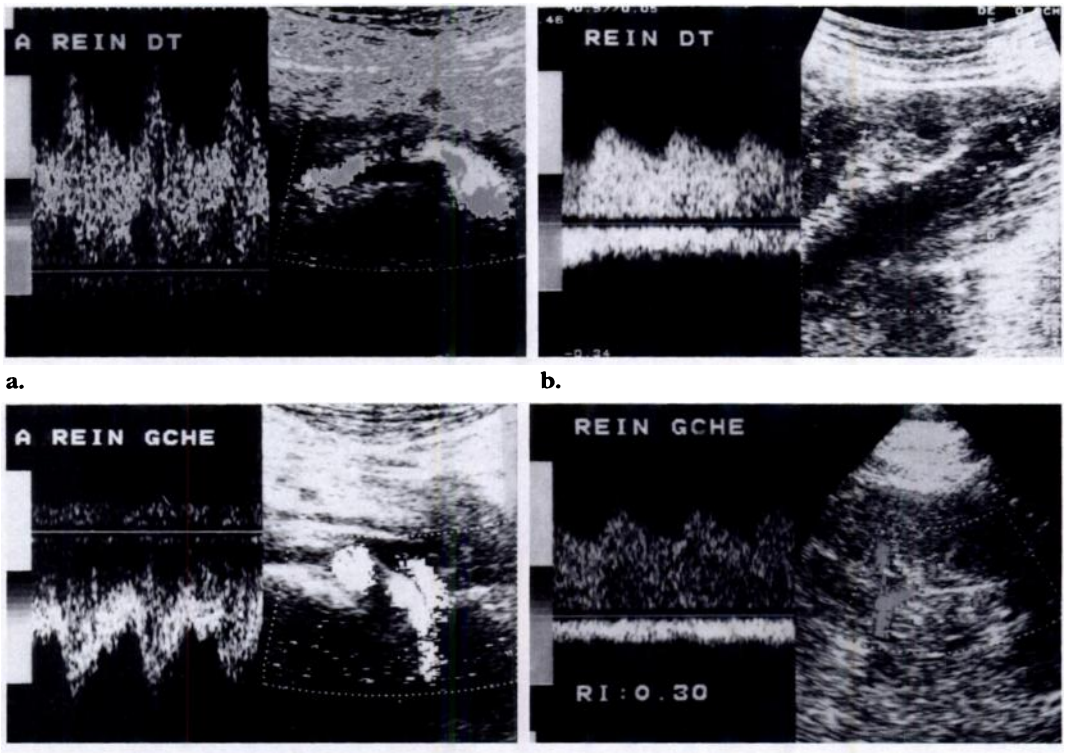

Figure 22. Coarctation of the aorta. **(a–d)** Doppler spectrum (left) and sonogram (right) demonstrate hemodynamic changes in the right **(a, b)** and left **(c, d)** kidneys and in the whole renovascular bed, including low-resistance waveforms and delayed and blunted systolic peaks in the intrarenal arteries **(b, d)**. Such findings are highly suggestive of a stenosis of the aorta upstream from the RAs. **(e)** Aortogram shows severe coarctation of the aortic arch (arrow).

e.

• Coarctation of the Aorta

In the one case of aortal coarctation in our series, spectral analysis of the main RAs demonstrated low resistance (RI < 0.50) and slightly turbulent waveforms in both kidneys with slowing and dampening of the systolic peak in the intrarenal arterial network (Fig 22). Concomitant alteration of aortic flow, including low resistance and more or less turbulent waveforms, suggested the diagnosis. Such congenital narrowing of the aorta should be considered in the differential diagnosis of renovascular hypertension because it may cause an increase in blood pressure in the upper extremities in young adults.

■ DISCUSSION

• RA Occlusive Disease

Although color Doppler US is noninvasive and inexpensive, the accessibility of the RAs to the ultrasound beam is a major limiting factor in evaluation of occlusive disease of the RA. Despite the poor results of some recent studies (12,13), in which the sensitivity of color Doppler sonography was as low as 0%, the addition

of the color Doppler technique is expected to increase the accuracy of Doppler US in the diagnosis of RA occlusive disease. In our experience, use of color Doppler flow imaging improves detection of the RAs, especially of supernumerary arteries, and facilitates identification of all segments of the RAs. Furthermore, color Doppler US allows direct visualization of hemodynamic changes, which in many cases strongly suggest the presence of a narrowed arterial segment prior to duplex Doppler interrogation.

Perivascular artifact appears to be much more uncommon in native kidneys with RA stenosis than in renal transplants with RA stenosis. Such artifact has not been previously reported in native kidneys, to our knowledge, but was observed in two cases of severe stenosis (5% of the total cases of stenosis) in our series.

When performed by an experienced operator, color Doppler US examination is technically successful in 75% of cases, including kidneys with multiple RAs. The sensitivity and specificity of color Doppler US are comparable with those of other noninvasive modalities, such as intravenous digital subtraction angiography (which has almost the same rate of technically inadequate studies). However, color Doppler US of the RAs is considered to be almost useless by some investigators (11–13) not only because of technical difficulties but also because it is time-consuming and highly operator-dependent. These limitations have prompted evaluation of downstream hemodynamic repercussions from the distal intrarenal arterial bed for indirect diagnosis of RA stenosis (14–16, 18–20). Such changes in the downstream arterial bed were noted by Kotval (21) in peripheral arteries in the form of the tardus-parvus waveform, representing a Doppler US sign of proximal flow obstruction.

Using distal Doppler waveform parameters (representing elements of the tardus-parvus phenomenon), prior investigators defined the following threshold values for RA stenosis (7,15–17): acceleration time, 0.07 seconds or longer; systolic acceleration, 3.0 m/sec^2 or less; RI < 0.56; and a lower pulsatility index with a side difference of 0.12 or more. Recently, Stavros and colleagues (16) reported promising results in diagnosis of significant (≥60%) RA stenosis using the above-mentioned parameters, particularly loss of the ESP (sensitivity, 95%; specificity, 97%; accuracy, 96%). One of the more relevant findings of Stavros et al was a 98% negative predictive value for Doppler US detection of 60% or greater stenosis when normal waveform morphology (with ESP) was found in segmental arteries. Conversely, Kliewer et al (19) found no statistically significant difference in Doppler parameters between stenotic and nonstenotic RAs or between nonstenotic RAs in hypertensive patients and nonstenotic RAs in normotensive patients.

Such discrepancies between the results of various studies may be due partly to inadequate sampling of peripheral arterial branches, including interlobar and arcuate arteries, since the diagnostic criteria should be defined solely on the basis of Doppler waveforms obtained from segmental arteries (16). Furthermore, most of these parameters may be influenced by vascular compliance changes and technical errors that result in false-positive results.

Although we did not consider numeric parameters in the diagnosis of RA stenosis, severe abnormalities in the shape of the Doppler waveform (ie, the tardus-parvus phenomenon defined qualitatively) obtained distally were among our criteria for detection of severely stenotic RAs.

The results of Kliewer et al (19) suggest that only the tardus-parvus phenomenon allows consistent discrimination between severely (≥80%) stenotic RAs and nonstenotic RAs. However, such changes are not always seen in critically stenosed arteries, as in four of 17 severely stenotic RAs in our series.

The presence of supernumerary arteries (which were responsible for approximately half of the false-negative results in the study of Kliewer et al [19]) and a well-developed collateral blood supply could explain the absence of tardus-parvus abnormalities in severe stenoses. In the three cases of severely stenotic single RAs without tardus-parvus abnormalities in our series, distal Doppler waveforms exhibited a marked decrease in RI, which may reflect the presence of a well-developed collateral blood supply or secondary changes in vascular compliance.

On the other hand, false-positive results (ie, tardus-parvus abnormalities distal to a nonstenotic main RA) could be due to technical factors (use of an improperly high velocity scale or pulsed Doppler power setting) or some pathologic conditions that may be associated with hypertension, such as distal atherosclerotic changes, arteriolonephrosclerosis, or vasculitis, which can affect intrarenal blood flow by changing vascular compliance or producing multiple distal stenoses. Our findings in three cases of distal occlusive disease suggest that the systolic component of Doppler waveforms obtained from interlobar arteries could be altered by such peripheral vascular lesions when the main RA is normal. The correct diagnosis may be suggested when intrarenal flow waveforms demonstrate bilateral inhomogeneous abnormalities, including tardus-parvus waveforms with concomitant accelerated and low-resistance flow from different arterial branches, especially when the main RAs have been successfully interrogated with color Doppler US. To our knowledge, this finding has not been reported in the literature.

As mentioned by Patriquin and colleagues (18), severe stenosis of the aorta upstream from the RAs may also affect intrarenal systolic curves in both kidneys and induce a marked decrease in resistivity in either the proximal or distal intrarenal arteries. To our knowledge, severe stenosis of the aorta is the only pathologic condition besides large bilateral AV fistulas that can substantially decrease RI values with normal systolic velocities in both main RAs. The latter entity should be easily identified because of intraparenchymal perivascular artifact and abnormal pulsatility of the vein.

Compared with RA stenosis, RA thrombosis is an uncommon cause of renovascular hypertension and may be associated with accelerated renal failure. Confident diagnosis of RA thrombosis requires color Doppler demonstration of two signs: (*a*) tardus-parvus abnormalities or absence of Doppler signal in the distal renal bed and (*b*) direct visualization of a mute RA. This diagnosis can be suggested only by analysis of waveforms from distal intrarenal vessels, since similar downstream abnormalities can be due to severe RA stenosis.

The majority of RA thromboses in our series (eight of 12 cases diagnosed with color Doppler US) demonstrated absence of an intrarenal arterial Doppler signal. Absent Doppler signal can result when an efficient collateral blood supply has not developed or when pulsed Doppler interrogation fails to obtain signal from intrarenal arterial branches. On the other hand, acute RA occlusion following renal trauma should demonstrate a complete lack of blood flow within the renal cortex, since efficient collateral blood supply does not develop under such circumstances. Therefore, color Doppler US may accurately detect such a complication whatever the technical result of Doppler interrogation of the proximal RA (successful or inadequate).

• RV Thrombosis

Color Doppler US appears to be particularly useful in the diagnosis of RV thrombosis because, in most cases, it allows accurate, noninvasive assessment of the RVs in patients with impaired renal function. RV thrombosis in native kidneys produces normal intrarenal venous signal and an irregular increase in arterial resistivity (22). On the other hand, RV thrombosis in renal transplants (which do not have the capacity for development of collateral venous supply) produces absence of intrarenal venous flow and highly resistive arterial spectra with retrograde flow during diastole (23,24). The diagnosis of RV thrombosis in native kidneys is therefore based solely on the detection of a mute RV, with an echogenic thrombus typically seen within the vein on color Doppler images. However, an anechoic or hypoechoic clot is likely to be present within the RV in early, acute RV thrombosis, since this finding has been reported in most other types of venous thrombosis, such as thrombosis of the lower extremities (25) or vascular accesses (26,27).

• AV Fistula

Color Doppler US appears to be the only noninvasive modality that enables detection of postbiopsy AV fistulas. Almost all AV fistulas seem to produce local tissue vibration from flow turbulence (28–30), allowing detection of the lesion on a color Doppler flow image obtained with an appropriate pulse repetition frequency setting (as low as possible). Congenital AV malformation, an uncommon pathologic condition, can also produce a perivascular artifact (28). Such a finding suggests the potential of color Doppler US as a noninvasive diagnostic tool for the detection of AV malformations responsible for chronic hematuria when results of excretory pyelography or CT are negative. Angiography is still mandatory—especially when color Doppler US suggests the presence of an

AV malformation—for making the final diagnosis and to determine if the lesion requires percutaneous transcatheter embolization. Further study of color Doppler US versus angiography is needed to establish whether angiography is still indicated when results of color Doppler US are negative in such cases.

• Peripheral Infarction

Although color Doppler US is valuable for detection of renal allograft necrosis (24), it seems to be less accurate for diagnosis of perfusion defects in native kidneys because of technical difficulties and particularly because of the deep location of such defects. Such technical problems and the small size of the infarct may prevent color Doppler US from demonstrating perfusion defects in native kidneys, resulting in false-negative studies. Large areas of infarction may be visible on a color Doppler image as a mute, hypoechoic area of cortex, similar to the appearance of an acute infarction in a renal transplant (24).

■ CONCLUSIONS

Color Doppler US appears to be effective in the diagnosis of renovascular disease. It is already the modality of choice for detection of acute RV thrombosis and postbiopsy AV fistula, particularly in patients with impaired renal function.

Although color Doppler US improves duplex Doppler identification of the RAs, including supernumerary arteries, the main limitation of this modality remains accessibility of the RAs to the ultrasound beam. Despite recent studies questioning the value of distal waveform parameters in the diagnosis of RA stenosis, we believe that proximal Doppler interrogation remains an important step in Doppler examination of the RAs. However, even when color Doppler US fails to demonstrate the proximal RAs, it still provides useful hemodynamic information on the distal renovascular bed. Normal morphology and normal velocity on waveforms obtained from intrarenal arteries allow exclusion of RA occlusion and most severe stenoses. Because of the extreme variability in the reported performance of color Doppler US between studies, further research is needed before color Doppler US can become widely accepted for routine evaluation of patients thought to have renovascular hypertension. We believe that, with standardization of technique and diagnostic criteria, color Doppler US will have a role in screening of high-risk patients for renovascular hypertension.

■ REFERENCES

1. Avasthi PS, Voyles WF, Greene ER. Noninvasive diagnosis of renal artery stenosis by echo-Doppler velocimetry. Kidney Int 1984; 25: 824-829.
2. Norris CS, Pfeiffer JS, Rittgers SE. Noninvasive evaluation of renal artery stenosis and reno-vascular resistance: experimental and clinical studies. J Vasc Surg 1984; 1:192-201.
3. Greene ER, Avasthi PS, Hodges JW. Non invasive Doppler assessment of renal artery stenosis and hemodynamics. JCU 1987; 15:653-659.
4. Dubbins PA. Renal artery stenosis: duplex Doppler evaluation. Br J Radiol 1986; 59:225-229.
5. Kohler TR, Zierler RE, Martin BS, et al. Non invasive diagnosis of renal artery stenosis by ultrasonic duplex scanning. J Vasc Surg 1986; 4: 450-456.
6. Robertson R, Murphy A, Dubbins PA. Renal artery stenosis: the use of duplex ultrasound as a screening technique. Br J Radiol 1988; 61: 196-201.
7. Handa N, Fukanaga R, Ogawa S, Matsumoto M, Kimura K, Kamada T. A new accurate and noninvasive screening method for renovascular hypertension: the renal Doppler technique. J Hypertens 1988; (suppl 4):S458-S460.
8. Taylor DL, Kettler MD, Moneta GL, et al. Duplex ultrasound scanning in the diagnosis of renal artery stenosis: a prospective evaluation. J Vasc Surg 1988; 7:363-369.
9. Zoller WG, Hermans H, Bogner JR, Hahn D, Middeke M. Duplex sonography in the diagnosis of renovascular hypertension. Klin Wochenschr 1990; 68:830-834.
10. Cornelis T, Postma CT, van Aalen J, de Boo T, Rosenbusch G, Thien T. Doppler ultrasound scanning in the detection of renal artery stenosis in hypertensive patients. Br J Radiol 1992; 65:857-860.
11. Kletter K, Mostbeck G, Duczak R. Captopril renography and duplex sonography: comparison of two noninvasive methods for the diagnosis and follow-up in renovascular hypertension. Contrib Nephrol 1990; 79:190-195.
12. Berland LL, Koslin DB, Routh WD, Keller FS. Renal artery stenosis: prospective evaluation of diagnosis with color duplex US compared with angiography. Radiology 1990; 174:421-423.

13. Desberg AL, Paushter DM, Lammert GK, et al. Renal artery stenosis: evaluation with color Doppler flow imaging. Radiology 1990; 177: 749-753.
14. Martin BS, Nanra RS, Wlodarczyk J, et al. Renal hilar Doppler analysis in the detection of renal artery stenosis. J Vasc Technol 1991; 15: 173-180.
15. Bardelli M, Jensen G, Volkmann R, Aurelli M. Non-invasive ultrasound assessment of renal artery stenosis by means of Gosling pulsatility index. J Hypertens 1992; 10:985-989.
16. Stavros AT, Parker SH, Wayne FY, et al. Segmental stenosis of the renal artery: pattern recognition of tardus and parvus abnormalities with duplex sonography. Radiology 1992; 184:487-492.
17. Tupler R, Kliewer MA, Carroll BA. Early systolic compliance peak/reflective-wave complex [letter]. Radiology 1993; 188:286.
18. Patriquin HB, Lafortune M, Jequier JC, et al. Stenosis of the renal artery: assessment of slowed systole in the downstream circulation with Doppler sonography. Radiology 1992; 184:479-485.
19. Kliewer MA, Tupler RH, Carroll BA, et al. Renal artery stenosis: analysis of Doppler waveform parameters and tardus-parvus pattern. Radiology 1993; 189:779-787.
20. Lafortune M, Patriquin H, Demeule E, et al. Renal arterial stenosis: slowed systole in the downstream circulation—experimental study in dogs. Radiology 1992; 184:475-478.
21. Kotval PS. Doppler waveform parvus and tardus: a sign of proximal flow obstruction. J Ultrasound Med 1989; 8:435-440.
22. Parvey HR, Eisenberg RL. Image-directed Doppler sonography of the intrarenal arteries in acute renal vein thrombosis. JCU 1990; 18:512-516.
23. Reuther G, Wanjura D, Bauer H. Acute renal vein thrombosis in renal allografts: detection with duplex Doppler US. Radiology 1989; 170: 557-558.
24. Hélénon O, Attlan E, Legendre C, et al. Gd-DOTA-enhanced MR imaging and color Doppler US of renal allograft necrosis. RadioGraphics 1992; 12:21-33.
25. Cronan JJ, Dorfman GS, Scola FH, et al. Deep venous thrombosis: US assessment using vein compression. Radiology 1987; 162:191-194.
26. Middleton WD, Picus DD, Marx MV, Melson GL. Color Doppler sonography of hemodialysis vascular access: comparison with angiography. AJR 1989; 152:633-639.
27. Dousset V, Grenier N, Douws C, et al. Hemodialysis grafts: color Doppler flow imaging correlated with digital subtraction angiography and functional status. Radiology 1991; 181:89-94.
28. Audigey I, Grenier N, Douws C, et al. Color Doppler flow imaging of congenital and postbiopsy intrarenal arteriovenous shunts. Rev Imagerie Med 1992; 4:385-390.
29. Middleton WD, Erikson S, Melson GL. Perivascular color artifact: pathologic significance and appearance on color Doppler US images. Radiology 1989; 171:647-652.
30. Middleton WD, Kellman GM, Melson GL, Madrazo BL. Postbiopsy renal transplant arteriovenous fistulas: color Doppler US characteristics. Radiology 1989; 171:253-257.

Invited Commentary

From:
Lincoln L. Berland, MD, Department of Radiology
University of Alabama at Birmingham, Birmingham, Alabama

In the preceding article, Hélénon et al do a commendable job of describing and illustrating vascular applications of color Doppler US. However, the glaring discrepancies in reported results with this technique have left many asking "Who do we believe?" and "How can we really use this technique?" I believe that more carefully analyzing the work reported in this and other articles may lead to some reasonable answers to these questions. To properly apply color Doppler US to renovascular diseases will require us to discriminate between those applications that truly remain controversial and those applications that are indeed validated by the work of Hélénon et al and other workers.

Color Doppler US has placed a great temptation before us. In many patients, we see the renal vasculature in precise detail and in its entirety with color Doppler US. Such cases are